ELEVENTH EUROPEAN ROTORCRAFT FORUM

Paper No. 85

A ROBUST GENERAL HELICOPTER TRIM PROGRAM

H. Azzam and P. Taylor

Department of Aeronautics and Astronautics
University of Southampton
Southampton, U.K.

September 10 - 13, 1985
London, England

THE CITY UNIVERSITY, LONDON, EC1V 0HB, ENGLAND

A ROBUST GENERAL HELICOPTER TRIM PROGRAM

H. Azzam, Research Fellow, Southampton University
P. Taylor*, Southampton Univeristy, U.K.

Abstract

Several aerodynamic and dynamic simplifications have been introduced in most of the reported helicopter trim methods. Meanwhile, the solution of the trim equations has been obtained by using a simple iteration scheme. This scheme hardly satisfies the mathematical condition for convergence. The objective of this paper is to present a general algorithm which provides a convergent solution for the trim problem. Non-uniform induced velocity profile and detailed aerodynamic data are used in the trim program to demonstrate that the general algorithm is capable of implementing arbitrary advanced mathematical models which simulate the various helicopter components.

Notation

a_o : Coning flapping angle relative to shaft axes, radians.
a_1 : Longitudinal disc tilt relative to shaft axes, positive backward, radians.
A_1 : Lateral cyclic control angle relative to shaft axes, positive for starboard movement of the control stick, radians.
b : Number of blades.
b_1 : Lateral disc tilt relative to shaft axes, positive starboard, radians.
B_1 : Longitudinal cyclic control angle relative to shaft axes, positive for forward movement of the control stick, radians.
c : Blade chord, metres.
g : Flap-wise mode shape, metres.
m : Mass per unit length of the blade, kilograms/metre.
M_h : Hub moment of individual blade, positive in the flapping up sense, Newtons-metre.
R : Rotor radius, metres.
θ_o : Collective pitch angle, radians.
θ : Feathering angle of the blade; $= \theta_o - A_1 \cos\psi - B_1 \sin\psi$, radians.
η : Time dependent coordinate of the flap-wise motion, radians.
ν : Natural flapping frequency ratio.

---

*presently Westland PLC, Yeovil, Somerset

1. Introduction

Several assumptions have been introduced in most of the reported helicopter trim methods in order to simplify the aerodynamic calculations; e.g. Stewart (1950, ref. 1), Price (1963, ref. 2), Keys (1979, ref. 3) and Ramos (1982, ref. 4). Furthermore, this simple aerodynamic representation justifies treating the lateral and longitudinal trim equations independently; Bramwell (1976, ref. 5). Nevertheless, these dynamic and aerodynamic simplifications are no longer needed because the high speed computer can allow the effective implementation of advanced mathematical models which describe the behaviour of the helicopter components much more adequately. This will result in a robust trim program. The computational costs of such a program necessitate a careful examination of the trim algorithm and its convergence.

In his thorough analysis, Price found that the various trim parameters are related through no less than fourteen non-linear equations. The problem of solving these equations at first sight seems a formidable task. Johnson (1980, ref. 6) stated that trimming the six forces and moments of the complete helicopter is a difficult problem, with convergence to the desired state by no means assured. This convergence problem arises from the simple iteration scheme used. This scheme is too sensitive to the initial values of the variables and hardly satisfies the mathematical condition required for convergence. The difficulty of attaining convergence increases when using a detailed model because a previously simple analytical equation is replaced by a set of complicated expressions. In reference 7 an alternative method has been developed. The Jacobian matrix of the partial derivatives has been constructed and used to update the values of the trim variables simultaneously. This scheme has been found to converge without difficulty throughout the conventional speed range with high accuracy. The analytical equations of reference 7 include some of the more significant higher order terms. Nevertheless, important aerodynamic details have been kept simple; for instant, a constant lift curve slope and drag coefficients have been assumed.

The purpose of this paper is to develop an efficient algorithm which can be utilized in a robust trim program by extending the above method. The objective is also to examine the versatility of this algorithm by implementing detailed aerodynamic data and an arbitrary non-uniform induced velocity profile. Also, a scheme based on the above procedure which provides a guaranteed convergence as long as the trim equations have real roots will be described.

2. The Overall Trim Equations

The steady state motion of a helicopter can be described by six equations which satisfy the equilibrium of the forces and moments of the vehicle components. For demonstration only, consider a single rotor helicopter whose fuselage forces and moments are known and its steady state mission is defined by specifying the velocity vector relative to a reference system of axes. Furthermore, assume that the main rotor pitching and rolling moments are proportional to the longitudinal and lateral disc tilt respectively, which is true as long as the first flap-wise mode shape only is considered. Then, the six equilibrium equations contain the following unknown parameters: the force and moment components of the main rotor, the thrust of the tail rotor and two angles which define the orientation of the helicopter relative to the reference axes. Thus, three equations have to be added to the equilibrium equations in order to determine the nine unknown trim variables. These equations may be obtained by expressing the main rotor forces as functions of the rotor parameters. By doing so, five extra variables, namely: the collective and cyclic control angles, the flapping coning angle and the induced velocity have been introduced. Therefore, an additional five equations are necessary in order to determine the fourteen unknowns. These five equations are: three for the components of the main rotor moment, one for the induced velocity and one for the coning flapping angle. In other words, the fourteen trim parameters are the force components of the main rotor and its torque, the flapping angles, the collective pitch angle, the cyclic control angles, the induced velocity, the tail rotor thrust and the fuselage attitude and bank angles. Meanwhile the fourteen overall trim equations can be obtained as follows:

- Six equilibrium equations.
- Four equations involving the thrust, in-plane force, side force and torque of the main rotor.
- The flapping equation from which three equations can be derived. Two of these equations may be considered as the equations describing the rolling and pitching moments of the main rotor and the third describing the coning flapping angle.
- One equation for the induced velocity profile.

The number of the trim parameters will increase when new components are introduced (e.g. wing, fin, horizontal tail plane and/or auxiliary forward thrust). Moreover, a comprehensive dynamic representation will add more variables, for example representing the lag motion of the blade about the drag hinge will introduce the drag angle as a new unknown.

3. The Solution of the Overall Trim Equations

In reference 7 the trim equations have been written in analytical form. The solution of the non-linear equations can be obtained as follows: If the overall trim equations have the form

$$F_i(X_1, X_2, X_3, \ldots\ldots X_n) = 0.0 \quad ,i=1,2,\ldots,n \tag{1}$$

where: "n" is the number of the equations.

Then the roots of these equations can be obtained iteratively from:

$$X_i(new) = X_i(old) + E_i \quad ,i=1,2,\ldots,n \tag{2}$$

where: "X_i" denotes the ith root and "E_i" is calculated from:

$$\begin{bmatrix} \partial F_1/\partial X_1 & \partial F_1/\partial X_2 & \partial F_1/\partial X_n \\ \partial F_2/\partial X_1 & \partial F_2/\partial X_2 & \partial F_2/\partial X_n \\ \ldots\ldots\ldots\ldots\text{etc}\ldots\ldots\ldots\ldots & & \\ \partial F_n/\partial X_1 & \partial F_n/\partial X_2 & \partial F_n/\partial X_n \end{bmatrix}_{X_i(old)} \begin{bmatrix} E_1 \\ E_2 \\ \ldots\ldots \\ E_n \end{bmatrix} = \begin{bmatrix} -F_1 \\ -F_2 \\ \ldots\ldots \\ -F_n \end{bmatrix}_{X_i(old)} \tag{3}$$

The basic feature of the above method is that the trim parameters (the roots) have been updated simultaneously. The method provides a solution to any required degree of accuracy in only a few iterations (typically 2 to 5 iterations). Moreover, the method avoids the sensitivity of the convergence to the initial values. As mentioned above, simplified assumptions have been introduced in order to be able to express the overall trim equations in analytical form.

Now, the above analytical scheme can be used to monitor the convergence of a more representative scheme which uses local blade aerodynamic data and a non-uniform induced velocity profile to calculate the main rotor forces and moments. In other words, the converging tendency of the simple model can be inherited by the detailed one. To illustrate this, consider the case in which the overall trim is described by fourteen equations. The six equilibrium equations have been derived with no small angle approximation. The remaining analytical equations describe the rotor forces and torque, the rotor flapping angles (a_o, a_1, b_1) and the momentum induced velocity. The induced velocity equation is removed from the above iterative procedure and the value of the average induced velocity used in the analytical equations is calculated once before the iteration starts. For given control angles (θ_o, A_1, B_1) and velocity state relative to the shaft axes (U_{xs}, U_{ys}, U_{zs}), the remaining seven analytical equations can be written as follows:

$$G_i(X_{a1}, X_{a2}, \ldots\ldots\ldots, X_{a7}) = 0.0 \qquad ,i=1,2,..,7 \tag{4}$$

where: The variables "X_{ai}" are the rotor forces, torque and flapping angles.

For the same control angles and velocity state relative to shaft axes, a more detailed rotor loads program will calculate different values for these variables; "X_i". Denoting the difference between "X_i" and "X_{ai}" by "C_i", equation (4) can be written as follows:

$$G(X_1 - C_1, X_2 - C_2, \ldots\ldots, X_7 - C_7) = 0.0 \qquad ,i=1,2,..,7 \tag{5}$$

Equation (5) means that the analytical equations can be forced to calculate accurate estimations which are exactly equal to the values calculated from a detailed program as long as the correction factors "C_i" are known. Thus the scheme of reference 7can be used to monitor the convergence by replacing equations (4) by (5) in the following iterative procedure:

(1) Specify the velocity state of the helicopter relative to reference axes; the input of the program is three velocity components which quantify horizontal, vertical and sideslip motion.
(2) Calculate a value for an average induced velocity to be used only in the analytical equations.
(3) Assign zero values to the seven correction factors "$(C_i)_{old}$".
(4) Use the analytical scheme to evaluate estimates for the thirteen trim parameters which are the main rotor forces and torque, the flapping angles, the orientation angles of the fuselage and the control angles. The fuselage orientation angles define the velocity state relative to the shaft axes of the main rotor.
(5) Use the current control angles and velocity state relative to the shaft axes as input to a detailed rotor loads program to calculate the main rotor forces, torque and the flapping angles. Denote the difference between the values of the seven parameters of the detailed program and those of the analytical equations by "ΔC_i".
(6) Update the values of the correction factors as follows:

$$(C_i)_{new} = (C_i)_{old} + \Delta C_i$$

(7) Repeat the procedure starting from step 4 until the differences between the results of the analytical solution and those of the detailed calculation are less than the specified precision ($\Delta C_i \rightarrow 0.0$).

Thus, the six equilibrium equations are satisfied. Meanwhile, the forces and moments used in these equations are obtained from a detailed rotor loads program whose velocity state input is defined by the orientation of the trimmed helicopter.

It is clear that a comprehensive dynamic representation of the rotor will require only the implementation of an appropriate rotor subprogram. Meanwhile the number of the trim parameters in the analytical equations remains the same. For example, considering the lag motion implies introducing the lag angle about the drag hinge in the rotor subprogram. This subprogram will calculate the average value of the torque to modify the associated analytical equation which can be derived for a rotor without lag degree of freedom. The analytical equations are only auxiliary equations which define the convergence criteria of a more comprehensive scheme.

The above scheme has been found to converge throughout the conventional helicopter speed range in 3 to 5 iterations. Nevertheless, more iterations are required for the operational conditions for which the rotor experiences a severe stall.

3. A Scheme for Guaranteed Convergence

The above scheme has been used successfully to trim conventional, winged and compound helicopters. Nevertheless, the convergence criteria is not mathematically rigorous. Therefore,

failure of the scheme to converge for a new configuration will raise doubts about both the mathematical procedure and the capability of the new configuration. The purpose of this section is to construct a scheme based on the above procedure which provides a guaranteed convergence as long as the overall trim equations have real roots. Thus, knowledge of whether the new configuration can perform its required mission or not may be obtained.

For arbitrary initial values of the variables, the following non-linear overall trim equations must be solved:

$$F_i(X_1,X_2,X_3,.....,X_n) = 0.0 \qquad ,i=1,2,...,n \tag{6}$$

(the factors "C_i" are implicitly included in the equations which describe the forces and moments of the various components of the helicopter)

An iterative scheme can be obtained by writing equation (6) in the following form:

$$X_i)_{new} = G_i(X_1,X_2,X_3,....,X_n) \qquad ,i=1,2,...,n \tag{7}$$

where: the values of the functions "G_i" are evaluated for the old estimates of the variables "X_i". This scheme will converge if

$$\sum_{i=1}^{n} \left| \partial G_j/\partial X_i \right| \; \langle \; 1 \qquad j=1,2,...,n \tag{8}$$

The functions "G_i" may be chosen as follows:

$$G_i = X_i + \sum_{j=1}^{n} a_{i,j} F_j \qquad ,i=1,2,...,n \tag{9}$$

Then the coefficients "$a_{i,j}$" can be selected such that the summations of the inequalities (8) are equal to zero, i.e.

$$\begin{bmatrix} \partial F_1/\partial X_1 & \partial F_2/\partial X_1 & \partial F_n/\partial X_1 \\ \partial F_1/\partial X_2 & \partial F_2/\partial X_2 & \partial F_n/\partial X_2 \\ \text{.....} & \text{etc} & \text{.....} \\ \partial F_1/\partial X_n & \partial F_2/\partial X_n & \partial F_n/\partial X_n \end{bmatrix} \begin{bmatrix} a_{i,1} \\ a_{i,2} \\ \text{.....} \\ a_{i,n} \end{bmatrix} = \begin{bmatrix} K_{i,1} \\ K_{i,2} \\ \text{.....} \\ k_{i,n} \end{bmatrix} ,i = 1,2,...,n \tag{10}$$

where: $K_{i,i} = -1$ and $K_{i,j} = 0.0$.

Thus, a scheme which guarantees a convergent solution as long as the roots of the equations are real can be derived by constructing a new set of non-linear equations each of them being a linear combination of the overall trim equations. The coefficients of each new equation are obtained by solving the corresponding set of linear equations given by (10) where the partial derivatives are evaluated for the initial values of "X_i".

4. Definition of the Axes Systems

The reference axes x_r,y_r and z_r are defined according to Figure 1. The z_r plane is horizontal. The x_r axis lies on the plane of symmetry of the helicopter and is pointing towards the helicopter nose. The origin "O" lies on the shaft axis. The velocity components of the helicopter U_{xr}, U_{yr} and

U_{zr}, will be referred to the reference axes since the mission of the helicopter is normally related to these axes.

The fuselage axes x_f, y_f and z_f are shown in Figure 1. The z_f plane is passing through the c.g. of the vehicle. The x_f axis lies on the plane of symmetry. Thus, the attitude angle "θ" and the bank angle; "Φ" will determine the position of the fuselage axes. The velocity components of the helicopter relative to the fuselage axes; U_{xf}, U_{yf} and U_{zf} are an essential input for the subprograms which calculate the fuselage, horizontal tail plane, fin and wing forces and moments. Denoting the unit vectors along the fuselage and the reference axes by i, j, k, i_r, j_r and k_r respectively. The transformation between the two systems becomes:

$$\begin{bmatrix} i \\ j \\ k \end{bmatrix} = \begin{bmatrix} \cos\theta & 0 & -\sin\theta \\ \sin\theta\sin\Phi & \cos\Phi & \cos\theta\sin\Phi \\ \sin\theta\cos\Phi & -\sin\Phi & \cos\theta\cos\Phi \end{bmatrix} \begin{bmatrix} i_r \\ j_r \\ k_r \end{bmatrix} \qquad (11)$$

The shaft axes x_s, y_s and z_s are defined in such a way that the line of intersection of the hub plane and the plane of symmetry is the x_s axis; Figure 2. Usually the rotor shaft is tilted forward to reduce the fuselage attitude angle at cruise. The transformation between the shaft axes and the fuselage becomes:

$$\begin{bmatrix} i_s \\ k_s \end{bmatrix} = \begin{bmatrix} \cos\gamma & \sin\gamma \\ -\sin\gamma & \cos\gamma \end{bmatrix} \begin{bmatrix} i \\ k \end{bmatrix} \qquad (12)$$

where i_s, j_s and k_s are unit vectors along the shaft axes. The above transformation is completely geometric. The velocity components of the helicopter relative to the shaft axes; U_{xs}, U_{ys}, U_{zs} are used as an input to the detailed rotor subprogram.

The most convenient axes to evaluate the rotor forces and moments are the rotor wind axes shown in Figure 3, especially when analytical equations are used to describe the rotor behaviour. These axes are defined such that the component of the velocity of the helicopter in the y_w direction vanishes. Hence the tansformation beween the wind axes of the rotor and the shaft axes becomes:

$$\begin{bmatrix} i_s \\ y_s \end{bmatrix} = \begin{bmatrix} U_{xs}/\sqrt{U^2_{xs} + U^2_{ys}} & -U_{ys}/\sqrt{U^2_{xs} + U^2_{ys}} \\ U_{ys}/\sqrt{U^2_{xs} + U^2_{ys}} & U_{xs}/\sqrt{U^2_{xs} + U^2_{ys}} \end{bmatrix} \begin{bmatrix} i_w \\ j_w \end{bmatrix} \qquad (13)$$

The above axes systems are only defined since they are independent of the mathematical models of each part of the helicopter. The fuselage axes which are fixed in the vehicle will be used in the trim analysis. Meanwhile, the shaft axes will be used for the rotor representation. These choices are justified as follows:

In the case of a helicopter, there is so much variation in the possible types of steady motion (e.g. forward, backward,sideways and vertical motion) that the complications arising with widely different moments and products of inertia rule out wind fuselage axes as a sensible choice for trim and stability investigations. The same argument rules out fuselage axes parallel to the rotor disc or the non-feathering axes. Therefore, fuselage fixed axes about which the moment of inertia of the vehicle are invariable, have been chosen. Furthermore, the relation between the chosen fuselage axes and the various components of the helicopter is only geometric.

The disc axes or the non-feathering axes have been frequently used in rotor models. The feathering axes allow for the disappearance of the control angles which are implied in the flapping response. Meanwhile, the disc axes allows for the disappearance of the first harmonic flapping coefficients which are implied in the control angles. The choice of one of these systems may simplify the aerodynamic analysis. However, inaccuracy and approximation will be incurred in the analysis For example the rotational speed of the rotor is about the shaft axis rather than the axis perpendicular to the swash plate or the tip-path plane. Furthermore, the elastic motion of the blade is more easily referred to the hub plane. The shaft axes is a logical choice for its accurate representation and direct incorporation into aeroelastic and stability investigations.

5. Helicopter Components Representation

For uncoupled out of plane motion, the modal equations are:

$$\ddot{\eta}_i + \Omega^2 \nu_i^2 \eta_i = \int \frac{\partial F}{\partial r} g_i \, dr / \int m g_i^2 \, dr \qquad (14)$$

where:

"g_i"	is the ith mode shape
"η_i"	is the ith time dependent coordinate (the flapping angle for the first mode shape)
"Ω"	is the rotational speed
"ν_i"	is the ith natural frequency ratio
"$\partial F/\partial r$"	is the aerodynamic load per unit span
"m"	is the mass per unit length

The hub moment can be calculated from the following equation:

$$M_h = \sum_i \left[\Omega^2 \left(\nu_i^2 - 1 \right) \eta_i \int m r g_i \, dr \right] \qquad (15)$$

where: "r" is the radial co-ordinate.

The pitching and rolling moments are proprotional to the longitudinal and lateral flapping angles when the first mode only is considered. Thus, a nose up tilt of the rotor disc relative to the hub plane will cause a nose up rotation of the fuselage.

The modal equation (14) can be solved by using a rapidly convergent technique based on curve fitting. For example, the flapping coefficients which are consistent with specified induced velocity profile and control angles have been calculated by solving a set of linear equations. These equations are obtained as follows:

An initial estimate of the flapping angle is used to calculate the aerodynamic moment about the flapping hinge at different azimuth stations around the disc. A damping coefficient is defined at each azimuth by dividing the damping part of the aerodynamic moment by the local derivative of the flapping angle. The flapping equation is rewritten such that the left hand side includes the damping coefficient multiplied by the derivative of the required flapping angle. The number of the coefficients of the Fourier expansion of the flapping angle is chosen to be equal to the number of the azimuth stations. The flapping equation is then satisfied at each azimuth station to give a set of linear equations. The solution of these equations provides a new estimate of the flapping coefficients. Any required precision can be obtained by repeating the above iterative technique.

The non-uniform induced velocity profile is obtained by using a prescribed wake model (ref. 8). The wake is allowed to contract and deflect. The strength of the tip vortex is related to the dynamic response of the blade. The three dimensional and blade vortex interaction effects have been accounted for simply. This model is found to predict the flapping angles (including the

lateral one), induced power, blade loadings and the induced velocities below the rotor adequately.

Hingeless bladed rotor

Young (1970,ref. 9) introduced the concept of the flapping hinge offset. Young's theory has been adopted ever since. Nevertheless, the hub moment per unit flapping angle calculated from Young's definition is less than that of equation (15). Also, this definition results in a high value of the equivalent flapping hinge offset especially for stiffer blades. As a result of that the aerodynamic moments about the equivalent flapping hinge offset will not represent the right hand side of equation (14). Furthermore, the local velocity due to the flapping will be in error especially near to the tip of the blade.

In the present work, the hub moment per unit flapping angle has been calculated from equation (15) by evaluating the natural frequency of the blade along with the integral of the equation from a blade flexibility analysis. The second integral of equation (14) has been calculated similarly. Then, the flapping hinge offset is defined such that the aerodynamic moment about the equivalent flapping hinge offset approximates the first integral of equation (14). Thus, better estimates of the flapping response and the hub moment result. The only source of inaccuracy is that due to the contribution of the flapping response to the local velocities of the air. However, because the new definition results in a smaller flapping hinge offset compared to that of Young, the prediction of these velocities will be improved especially in the important tip region.

At high forward speed one mode is no longer sufficient. Simons (1970, ref. 10) and Curtiss and Shupe (1971, ref. 11) found that a number of modes which, in superposition, approximate to the true loading shape has to be introduced in order to obtain an accurate estimate of the hub moment from equation (11). They suggested the following formula which require one or two modes only:

$$M_h = \int \frac{\partial F}{\partial r} r\, dr \qquad (16)$$

The above formula is derived to calculate better estimates of the pitching and rolling moments but not to calculate the hub moment itself.

Fuselage

The variation of the fuselage forces and moments with its orientation relative to the free stream is primarily due to the fuselage induced flow. A mathematical model which may simulate the fuselage should be based on the panel method (potential theory) and boundary layer theory coupled together; this requires large additional computational costs. Alternatively, previous wind tunnel tests for somewhat similar configurations can be used (references 12 and 13). In this case a careful interpretation of the data is required. For example, the data of reference 13 is for a model fuselage including horizontal tail plane. A considerable part of the pitching moment is due to the stabilizer. Meanwhile the size and setting angle of the tail plane are important trim and stability parameters. For this reason, the horizontal tail plane is treated separately. The fuselage down load can be calculated by the method presented in reference 4.

Lifting Surfaces

The panel method or lifting surface theory can be used in this case. Such a representation will be very useful to investigate the induced loads due to the rotor tip vortex interactions with the lifting surfaces. Nevertheless, for design purposes and day to day work, it is sufficient to calculate an average value of the forces and moments. Therefore, simple models based on the theory of reference 14 and 15 may be used. Meanwhile the effect of the induced flow of the main rotor and tail rotor may be accounted for by an average induced flow over the surfaces. The geometry,

location and setting angles of the horizontal tail plane, wing and fin are input parameters in the trim program.

6. General Discussion

The Glauert induced velocity profile as well as that of the prescribed wake model described above have been used in the trim analysis. The difference between these profiles is examined by calculating the lateral flapping angle for a model rotor; Figure 5. The results of the prescribed wake model are reasonably good compared to the experimental data of Harris (1972, ref. 16). Meanwhile, the results of the Glauert wake are found to be better than those of the theoretical models presented in reference 16. Reasons for this can be traced to the implementation of two dimensional aerofoil data, the accurate calculation of the local velocities of air (the small angle approximation having been removed) and the simple account of the three dimensional effects (see reference 8).

Figures 6 to 17 show the trim parameters of a conventional helicopter in forward flight (case 1, table 1). As expected, the power is more representative when using the prescribed wake model; figure 6. Severe stall can be observed at an advance ratio of 0.4 corresponding to forward speed of 84.5 m/s (164.1 knots). A complete consistency between the induced velocity profile and all of the flapping harmonics are required in order to locate the advance ratio at which such a phenomenon starts. Moreover, the unsteady effects have to be introduced. Figures 7 to 9 show the rotor forces relative to the shaft axes. The control angles variation with speed are shown in figures 10 to 12. It is clear that the peak of the lateral flapping angle at low speed (figure 5) is suppressed by a peak in the lateral cyclic control in order to maintain the moment balance. The flapping angles relative to the shaft axes are shown in figures 13 to 15. Both induced velocity profiles produce approximately the same first harmonic flapping coefficients to provide the same values of the pitching and rolling moments required for trimming the vehicle. The fuselage attitude and bank angles are shown in figures 16 and 17. The aforementioned figures indicate that the Glauert wake is quite capable of describing the features of the trim parameters.

Zero attitude angle at cruise speed can be achieved by a forward tilt of the rotor shaft; figure 18. The effect of the forward shaft tilt on the fuselage bank angle is shown in figure 19 in order to demonstrate the effect of solving the coupled trim equations. The bank angle can be controlled by a small sideslip velocity or by a sideway tilt of the shaft.

Although, the trim program solves the fully coupled trim equations and the phase between the flapping and cyclic control is not exactly 90 degreees, the mechanism of generating the rotor forces and moments may be interpreted as follows: A movement of the control stick causes tilt of the rotor disc, and in-plane force and moment in the same sense of this movement. For example, a forward tilt of the swash plate (an increase in the longitudinal cyclic control angle will cause a forward tilt of the rotor disc (a reduction in the longitudinal flapping angle) and hence, a nose down pitching moment and a H-force which is pointing forward (negative H-force).

Now, a forward movement of the c.g. results in a nose down pitching moment. Thus a backward tilt of the rotor disc is required to balance this moment. The backward tilt of the disc causes an increase in the H-force, hence a forward tilt of the fuselage is required to balance this force. The backward tilt of the disc can be obtained by a backward tilt of the swash plate (i.e. by reducing the longitudinal cyclic control); figures 20 to 23.

The high positive values of the longitudinal cyclic control angle is the prime reason of the onset of the retreating blade stall (case 1). The forward tilt of the swash plate is the available control to provide nose down pitching moment (i.e. to suppress the backward tilt of the rotor disc). Thus, if the setting angle of the horizontal tail plane is adjusted to provide sufficient nose down pitching moment, the forward tilt of the swash plate will be reduced and the retreating blade stall will be delayed; figures 24 to 28 (case 2). As mentioned above, this will be accompanied by an increase in the H-force and hence, an increase in the forward tilt of the fuselage. Therefore, the setting angle of the horizontal tail plane and its size are design parameters not only for the stability of the helicopter but also for its performance.

An increase in the tip speed of the rotor reduces the asymmetry of the flow field around the rotor disc at a given forward speed. Consequently, the backward tilt of the uncontrolled rotor will be reduced. Thus, the forward tilt of the swash plate required to suppress the disc tilt will be reduced and the stall will be delayed. In figures 24 to 28 (case 3) the increased tip speed along with the horizontal tail plane parameters are used to extend the forward speed up to 91.4 metres/second (177.5 knots).

The blade tip sections on the advancing side suffer from unfavourable Mach number effects at high speed. In this case, a forward tilt of the swash plate is required to reduce the angle of attack on the advancing side. Obviously, this will cause the onset of the retreating blade stall. Alternatively, a reduction in the collective pitch angle is required. Off loading of the rotor can be achieved by increasing the setting angle of the horizontal tail plane and its size or by introducing a wing. Nevertheless, off loading of the helicopter rotor requires a forward fuselage tilt to provide a propulsive force, and hence an increase in the collective pitch angle is expected to maintain the rotor thrust at the required level. Moreover, the tilt of the fuselage results in an incremental nose up pitching moment of the fuselage and the stabilizer, hence a forward movement of the control stick is required to balance this moment. Thus the extension of the speed of a winged helicopter will be limited. Adding a forward auxiliary propulsive system eliminates the need for the fuselage tilt. In this case, the rating of the propulsive system and its setting angles are new design parameters. Figures 24 to 28 (case 4 and 5) show the basic features of two compound helicopters. The maximum forward speeds are 101.4 and 97.2 m/se (197 and 188.7 knots).

The capability of the trim algorithm to find a unique physical solution of the trim equations for arbitrary detailed models has been demonstrated. Perhaps, mathematical uncertainty of the solution near to the severe stall boundary will arise because of the possibility of the existence of two solutions (for the simple case of two dimensional aerofoil, there are two angles of attack which give the same lift near the stall boundary). However, monitoring the progress of the iteration showed that the uncertainty is limited to a narrow region, therefore the speed at which the severe stall occurs is so near to that observed by the trim program. Besides, limits such as the available power are expected to stop the program well before this boundary.

Concluding Remarks

A robust helicopter trim program has been developed which provides a convergent solution normally within a few iterations. The capability of this program has been demonstrated by including a non-uniform induced velocity profile and local blade aerodynamics within the rotor force and moment representation. More complicated mathematical models which simulate the helicopter components more realistically, can be incorporated into the trim program without violating the convergence tendency.

Table 1

Brief description of the helicopter configurations

AUW = 40000.0 Newtons, b = 4, R = 6.402 metres, c = 0.39 metres, U_{yr},U_{zr} = 0.0

Case No.	:	1	2	3	4	5
Ω, radians/seconds	:	33	33	34	33	33
Stabilizer area, metres	:	0.4	0.4	1.2	1.0	0.4
Stabilizer setting angle, degrees	:	-I.55	11.5	14.3	9.4	0.0
Wing area, metres	:	-	-	-	-	3.0
Wing setting angle, degrees	:	-	-	-	-	11.5
Wing aerodynamic centre location	:	-	-	-	-	-0.03
Forward thrust/fuselage drag	:	-	-	-	1.0	0.6

Appendix "A"

the equilibrium equations of the helicopter

Referring to the definitions of figures 1, 2 and 4 the equilibrium equations of the helicopter relative to the fuselage axes become:

$$-W\sin\theta - H\cos\gamma + T\sin\gamma + R_x = 0 \qquad (A.1)$$

$$W\cos\theta\sin\Phi - Y + T_t + R_y = 0 \qquad (A.2)$$

$$W\cos\theta\cos\Phi - H\sin\gamma - T\cos\gamma + R_z = 0 \qquad (A.3)$$

$$y_g W\cos\theta\cos\Phi + z_h Y + M_r\cos\gamma - Q\sin\gamma - z_t T_t + M_x = 0 \qquad (A.4)$$

$$-x_g W\cos\theta\cos\Phi + x_h(H\sin\gamma + T\cos\gamma) + z_h(T\sin\gamma - H\cos\gamma) + M_p + M_y = 0 \qquad (A.5)$$

$$x_g W\cos\theta\sin\Phi + y_g W\sin\theta - x_h Y + M_r\sin\gamma + Q\cos\gamma + x_t T_t + M_z = 0 \qquad (A.6)$$

where:

H	:	Main rotor H-force, positive backwards
M_p	:	Main rotor pitching moment, positive nose up
M_r	:	Main rotor rolling moment, positive starboard
M_x,M_y,M_z	:	Moments of other parts of the helicopter
Q	:	Main rotor torque, positive clockwise
R_x,R_y,R_z	:	*Forces of other parts of the helicopter*
T	:	Main rotor thrust, positive upward
T_t	:	Tail rotor thrust, positive starboard
x_g,y_g	:	Components of the position vector of the c.g.
x_h,z_h	:	Components of the position vector of the hub centre
x_t,y_t,z_t	:	Components of the position vector of the tail rotor centre
θ	:	Fuselage attitude angle, positive nose up
Φ	:	Fuselage bank angle, positive starboard
γ	:	Shaft tilt, positive forward

References

(1) W. Stewart — Helicopter Control toTrim in Forward Flight ARC R&M 2733 March 1950.

(2) H.L. Price — Rotor Dynamics and Helicopter Stability, Aircraft Engineering, March to December 1963, March and April 1964 and November 1965.

(3) C.N. Keys — Rotary-Wing Aerodynamics, Vol. II, NASA CR 3083, 1979.

(4)	O.R. Ramos	Helicopter Computer Aided Design, MOD Research Agreement ERC/9/4/2040/0225XR/STR, 1983.
(5)	A.R.S. Bramwell	Helicopter Dynamics, Edward Arnold, 1976.
(6)	W. Johnson	Helicopter Theory, Princeton University Press, 1980.
(7)	H. Azzam	Investigation of Rotor Wing Interference, M.Sc. Thesis, Southampton University, March 1980.
(8)	H. Azzam and P. Taylor	Investigation of Helicopter Twin-Tail Rotor Characteristics, Southampton University, ASSU Memo 83/6, 1983.
(9)	M.I. Young	A Simplified Theory of Hingeless Rotors with Application to Tandem Helicopter, 18th Annual National forum of the AHS, 1962.
(10)	I.A. Simons	Some Thoughts on a Stability and Control Research Programme with Special Reference to Hingeless Rotor Helicopter, WHL Res. Memo 79, 1970.
(11)	H.C. Curtiss and N.K. Shupe	A Stability and Control Theory for Hingeless Rotor, 27th Annual National Forum of the AHS, 1971.
(12)	J.C. Biggers., J.L. McCloud and P. Patterakis	Wind-Tunnel Tests of Two Full-Scale Helicopter Fuselages, NASA TND-1548, October 1962
(13)	G.E. Sweet and J.L. Jenkins	Wind-Tunnel Investigation of the Drag and Static Stability Characteristics of Four Helicopter Fuselage Models, NASA TND 1363, July 1962.
(14)	S.F. Hoerner	Fluid-Dynamic Drag, Published by the Author, 1965.
(15)	S.F. Hoerner and H.V. Borst	Fluid-Dynamic Lift, Published by Mrs. Hoerner, 1975.
(16)	F.D. Harris	Articulated Rotor Blade Flapping Motion at Low Advance Ratio, Journal of the AHS, January 1972.

Acknowledgement

The support of Procurement Executive, Ministry of Defence, is gratefully acknowledged.

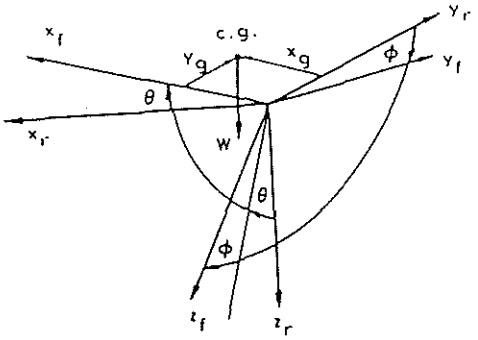

FIG. 1

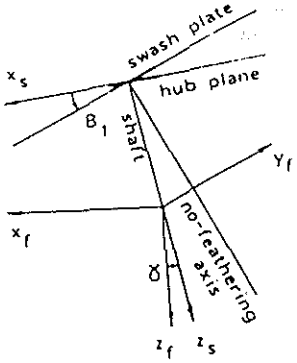

FIG. 2

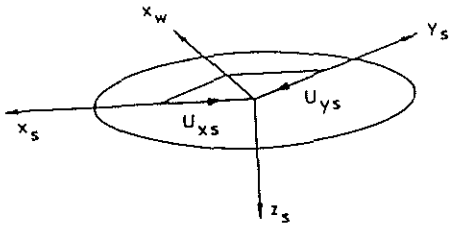

FIG. 3

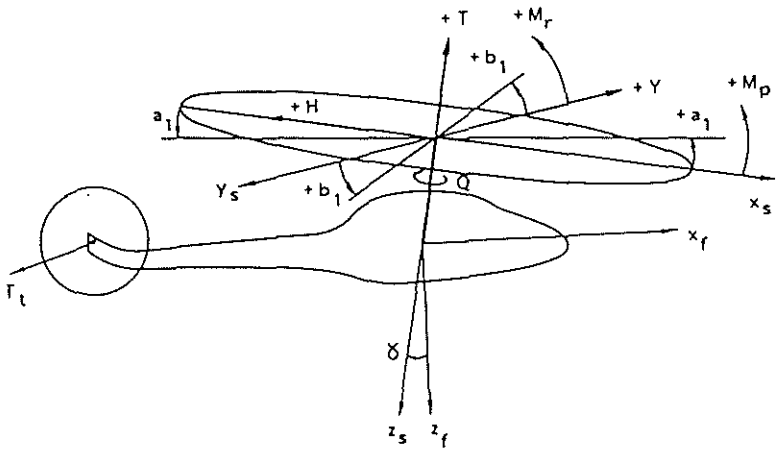

FIG. 4

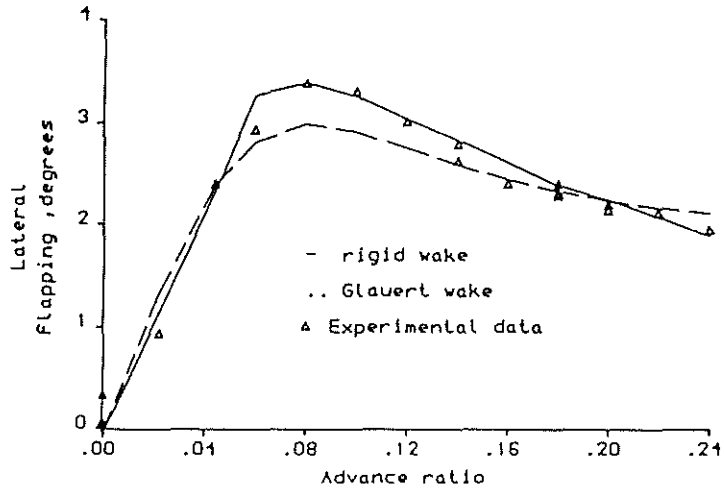

FIG.5 LATERAL FLAPPING IN FORWARD SPEED

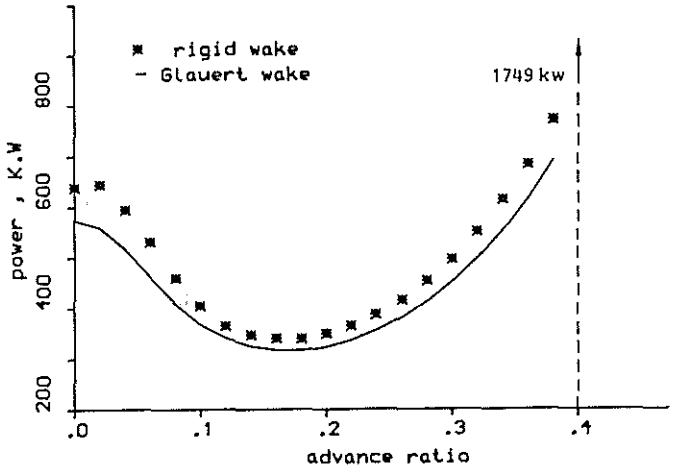

FIG.6 ROTOR POWER IN TRIMMED FLIGHT

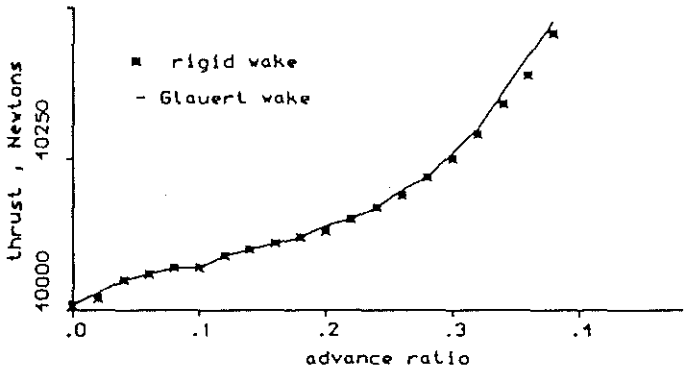

FIG.7 ROTOR THRUST IN TRIMMED FLIGHT

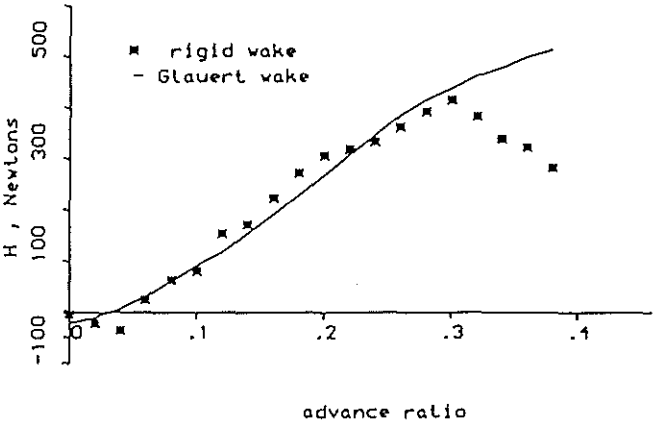

FIG.8 ROTOR H-FORCE IN TRIMMED FLIGHT

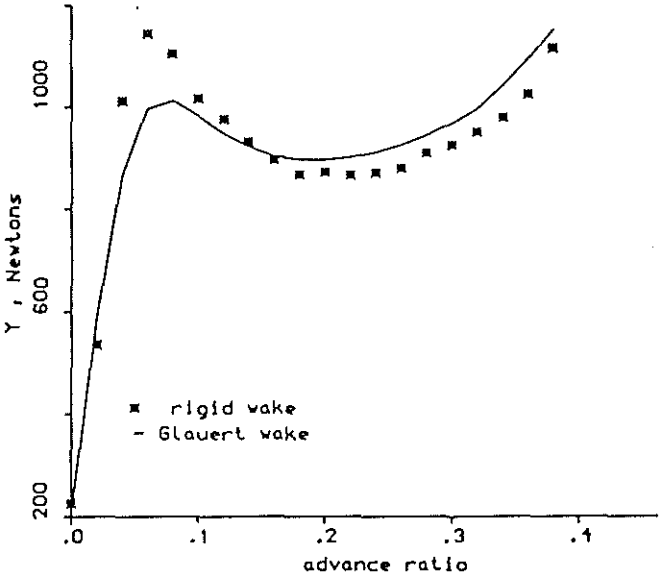

FIG.9 ROTOR Y-FORCE IN TRIMMED FLIGHT

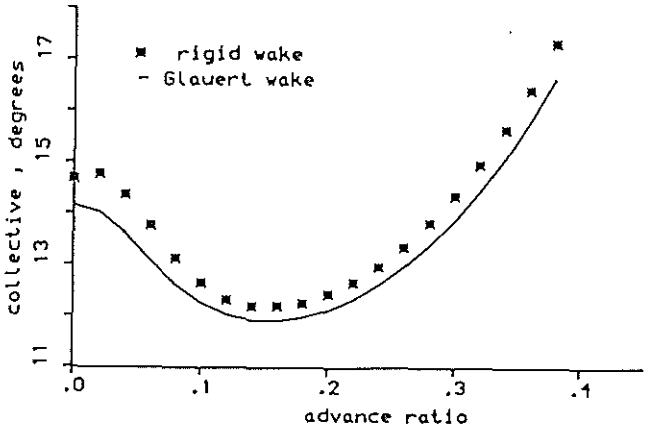

FIG.10 COLLECTIVE PITCH ANGLE TO TRIM

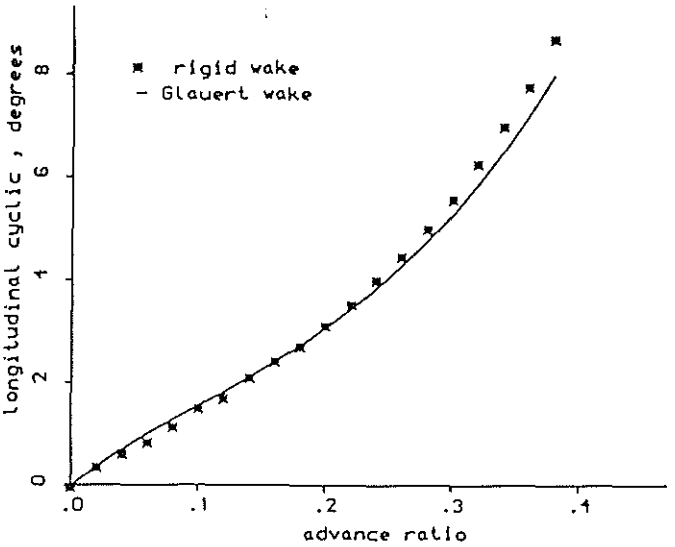

FIG.11 LONGITUDINAL CYCLIC CONTROL TO TRIM

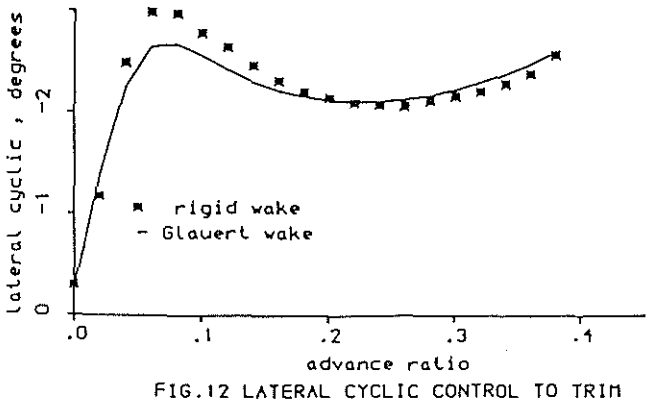

FIG.12 LATERAL CYCLIC CONTROL TO TRIM

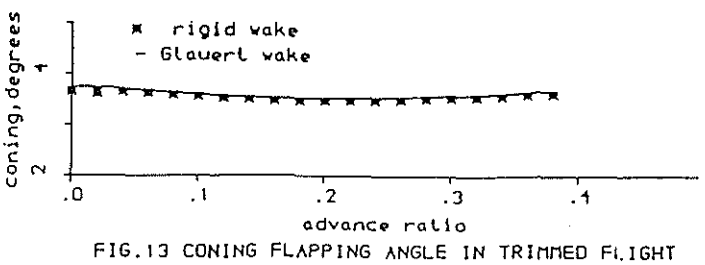

FIG.13 CONING FLAPPING ANGLE IN TRIMMED FLIGHT

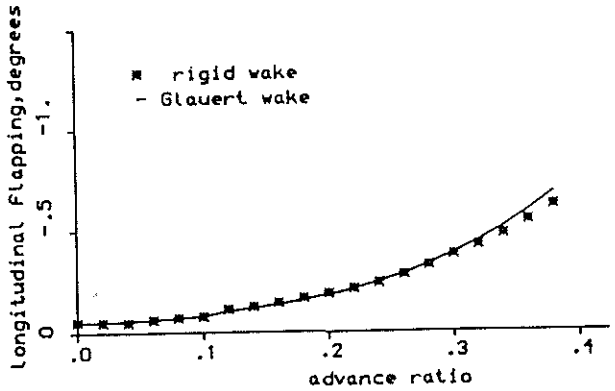

FIG.14 LONGITUDINAL FLAPPING ANGLE IN TRIMMED FLIGHT

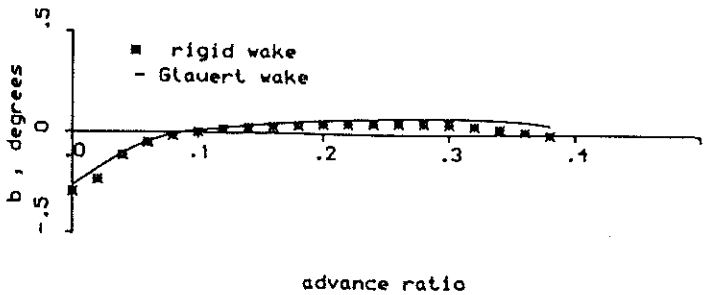

FIG.15 LATERAL FLAPPING ANGLE IN TRIMMED FLIGHT

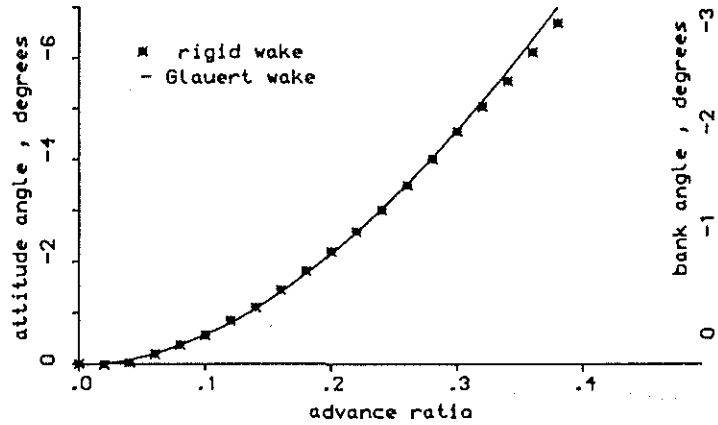

FIG.16 FUSELAGE ATTITUDE ANGLE IN TRIMMED FLIGHT

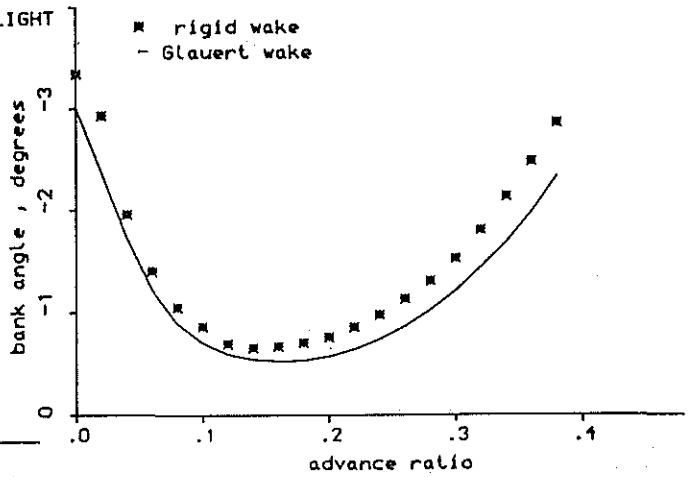

FIG.17 FUSELAGE BANK ANGLE IN TRIMMED FLIGHT

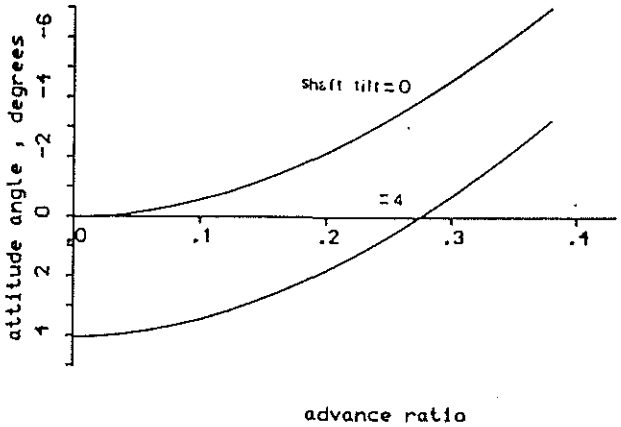

FIG.18 EFFECT OF SHAFT TILT ON THE ATTITUDE ANGLE

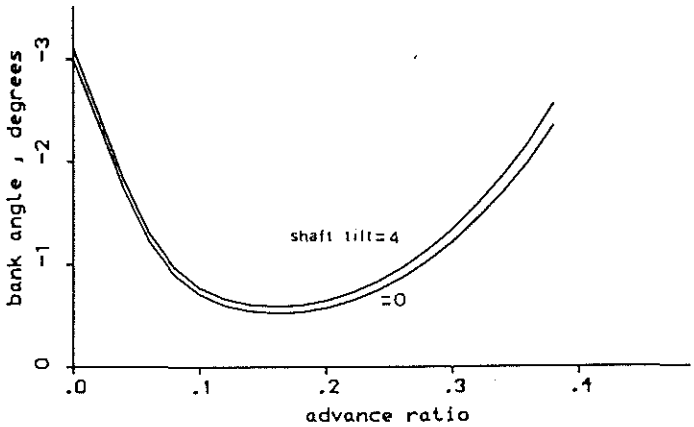

FIG.19 EFFECT OF SHAFT TILT ON THE BANK ANGLE

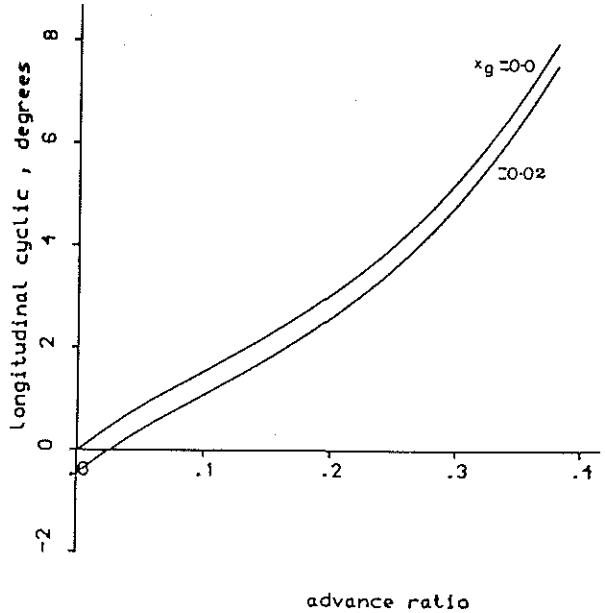

FIG.20 EFFECT OF C.G POSITION ON THE LONGITUDINAL CYCLIC

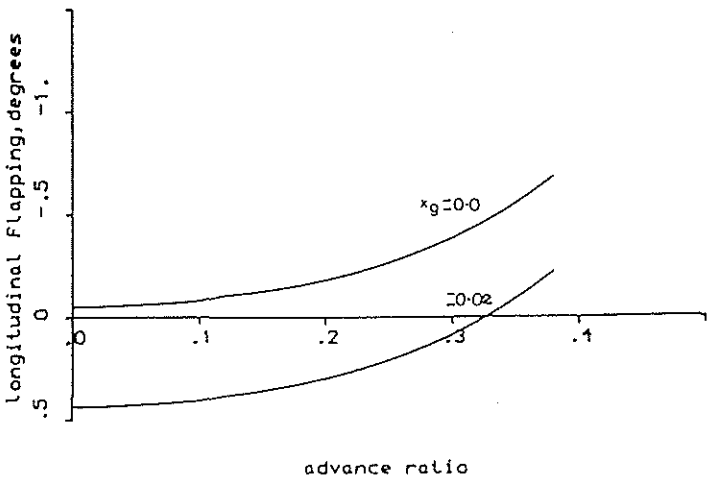

FIG.21 EFFECT OF C.G POSITION ON THE LONGITUDINAL FLAPPING

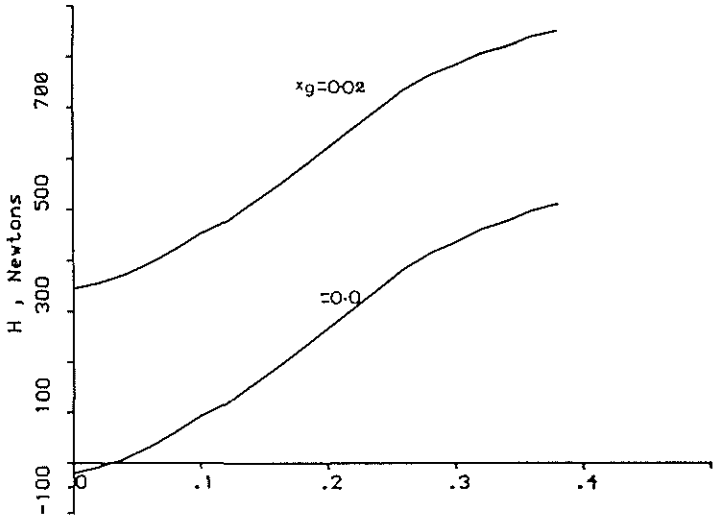

FIG.22 EFFECT OF C.G POSITION ON THE H-FORCE

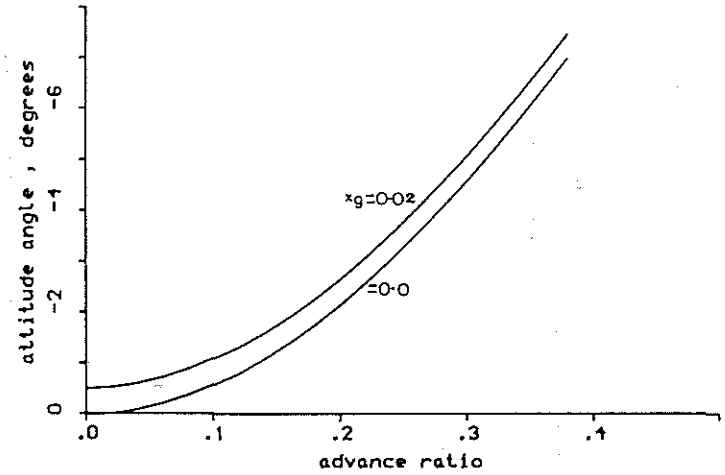

FIG.23 EFFECT OF C.G POSITION ON THE ATTITUDE ANGLE

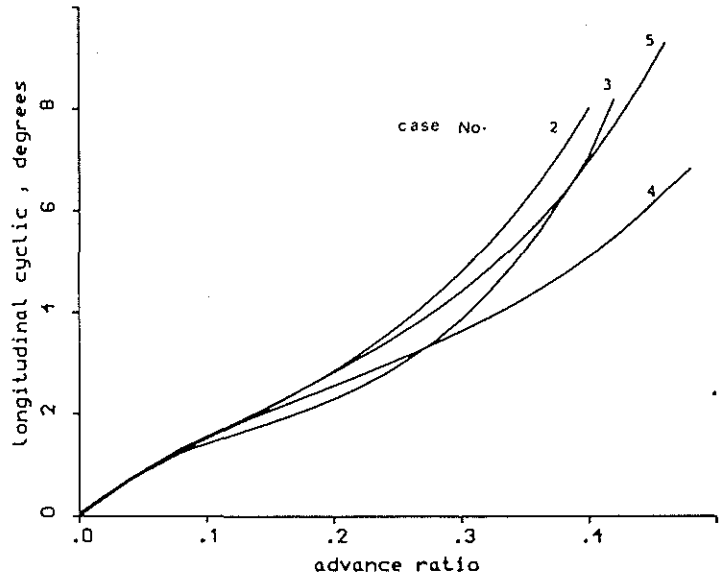

FIG.24 LONGITUDINAL CYCLIC CONTROL TO TRIM

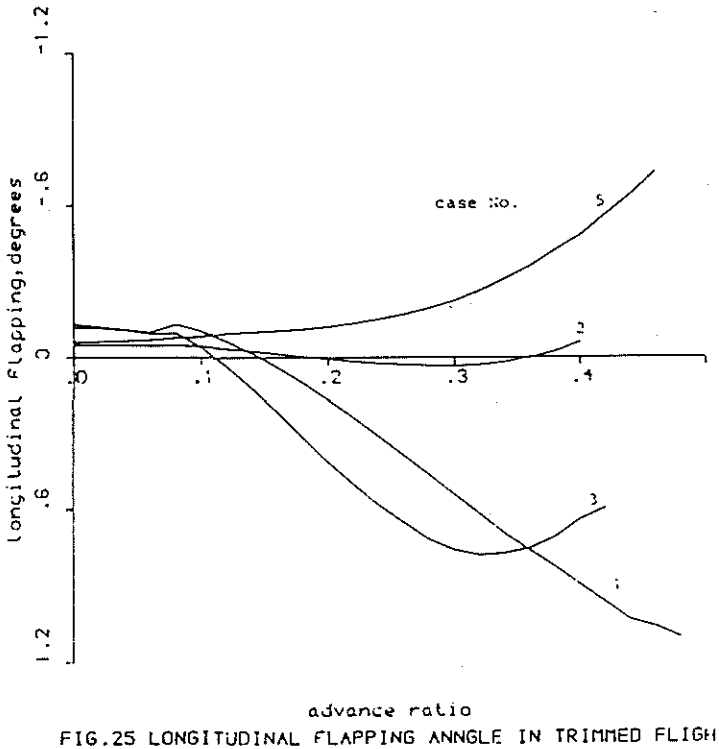

FIG.25 LONGITUDINAL FLAPPING ANNGLE IN TRIMMED FLIGH

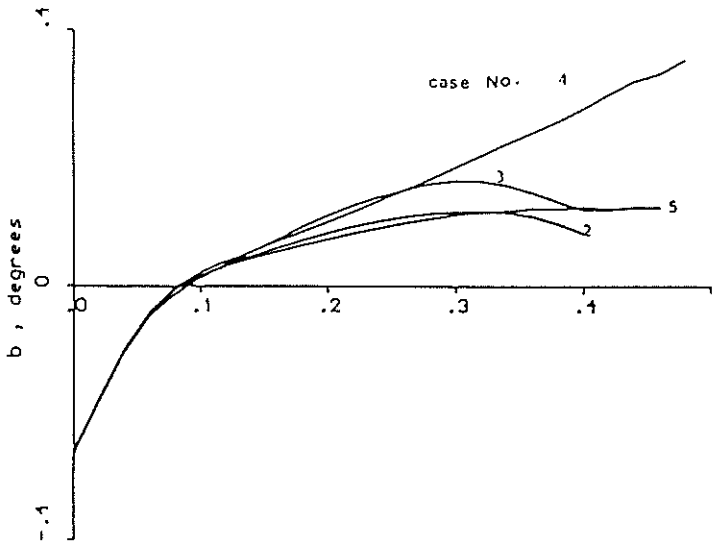

FIG.26 LATERAL FLAPPING ANGLE IN TRIMMED FLIGHT

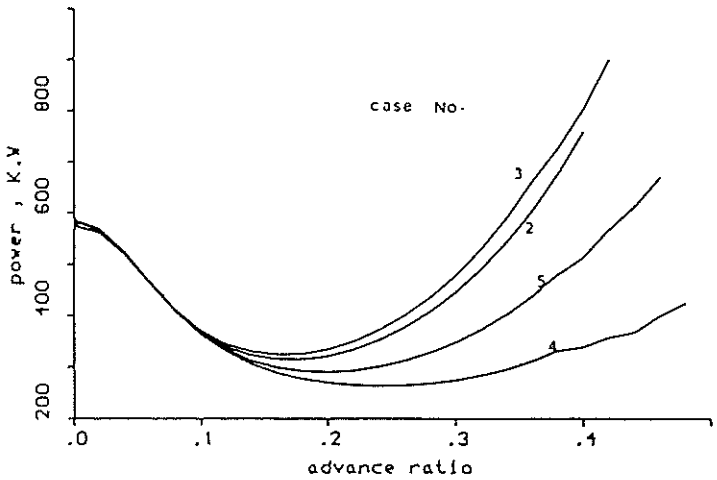

FIG.27 ROTOR POWER IN TRIMMED FLIGHT

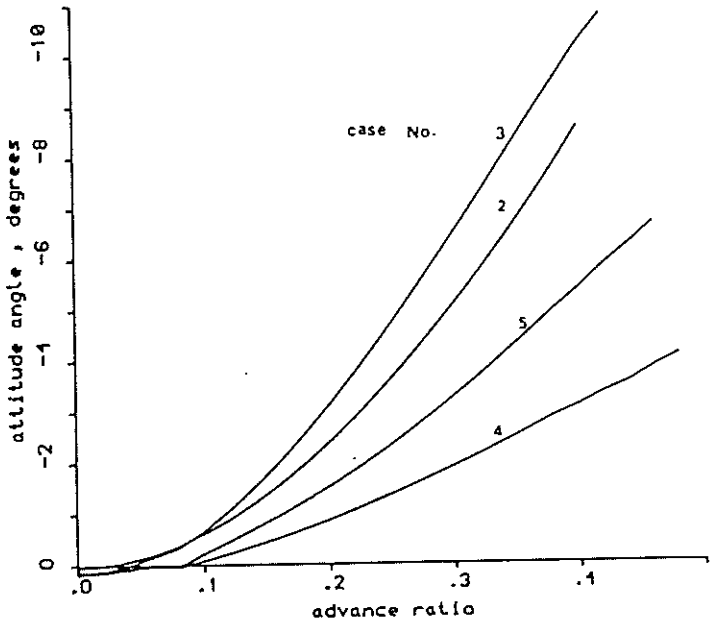

FIG.28 FUSELAGE ATTITUDE ANGLE IN TRIMMED FLIGHT